JOURNAL OF Materials CHEMISTRY

An X-ray absorption spectroscopic study on the local environment of copper in CuAPO-5

David G. Nicholson and Merete H. Nilsen*

Department of Chemistry, Norwegian University of Science and Technology (NTNU), N-7491 Trondheim, Norway

Received 31st January 2000, Accepted 8th June 2000
Published on the Web 17th July 2000

A copper-containing $AlPO_4$-5 was synthesised using copper(II) oxide as the copper source and tetraethylammonium hydroxide as the template. The local environment about copper in the as-synthesised, calcined and hydrogen-reduced materials has been studied using XANES and EXAFS. The results for the as-synthesised product show that copper is sited within the $AlPO_4$-5 framework and that its local environment is a tetragonally distorted $Cu(O)_6$ octahedron in which the axial bonds are possibly to hydroxy groups. On calcining at 550 °C the environment changes to a non-tetragonally distorted octahedron for which the coordination to the framework is increased by two long bonds to framework oxygens. Copper(II) in CuAPO-5 is reduced by 5% H_2 in He to copper particles of dimensions >40 Å. The catalytic properties of two CuAPO-5 samples (derived from copper(II) oxide and, for comparison, from copper(II) acetate) in the selective catalytic reduction of NO in the presence of NH_3 and O_2 have been investigated, showing maximum conversions of 27% at 440 °C and 53% at 340 °C, respectively.

Introduction

Zeotypic structures (zeolites and aluminophosphates) can incorporate metal atoms in several ways:

(1) metal atoms can bind to the internal surfaces that define the channels as well as to the external surfaces.
(2) certain metals can substitute for a small fraction of the central atoms within the framework (*i.e.* aluminium and also phosphorus in the case of the AlPOs).
(3) attachment by ion exchange is a characteristic feature of the zeolites because of their charged lattices.

Framework substitution of AlPOs occurs for a number of metals such as Li, Be, B, Mg, Si, Ti, V, Cr, Mn, Fe, Co, Ni, Zn, Ga, Ge, As, Zr and Sn.[1–11] An apparent exception is copper, for which the literature reports several unsuccessful attempts to incorporate copper into AlPO-frameworks (*e.g.* Rajic *et al.*[12]). Moen *et al.*[13] explained this for syntheses involving the secondary and tertiary amine templates, dipropylamine (DPA) and triethylamine (TEA). They found that copper(II) is reduced to copper(I) by these templates at temperatures above 190 °C. Under these conditions, and in the absence of coordinating anions (*e.g.* Cl^-), copper(I) disproportionates to metallic copper and copper(II), thereby preventing uptake of copper(II) into the framework. In addition, although these amines do not reduce copper(II) below 190 °C they still prevent the incorporation of copper into the lattice by forming stable complexes with copper(II).

Clearly, molecules possessing templating properties, but which do not complex copper(II), are of interest in syntheses aimed at incorporating copper(II) into AlPOs. Obvious candidates are quaternary amines because they are not Lewis bases yet at the same time can behave as templates. With this in mind, we have studied the use of the quaternary amine tetraethylammonium hydroxide (TEAOH) as the template in the synthesis of copper–AlPO systems. The results of similar work have recently been reported by Muñoz *et al.*[14] who described a synthesis of CuAPO-5. From structural studies (XRD, FT-IR, ESR and ESEM) they concluded that 3 wt% copper is sited on framework positions. They also suggest that copper specifically substitutes for phosphorus rather than aluminium.

Interest in catalytic and shape selective properties of metal incorporated zeotypes has given rise to a number of studies.[15–17] Since the active sites within these catalysts often contain substituted metal atoms, much of this attention has been directed towards identifying their modes of attachment. In particular, the catalytic activity of copper-containing materials in the removal of nitrogen oxides (NO_x) has been much studied.[18–20] A well known method for removing NO_x from stationary sources involves the reduction of NO by NH_3 in the presence of O_2.[21] In this connection the copper-ion exchanged zeolites H-ZSM-5[22] and H-mordenite[23] have attracted attention. These have certain advantages over a commonly used non-zeotypic catalyst, V_2O_5/TiO_2.[22,24] Copper-containing zeotypes other than the ion-exchanged materials may also be interesting candidates, for example CuAPOs. Since these are new materials any catalytic behaviour has not yet been established.

X-Ray absorption spectroscopy (XAS) is a widely used method for characterising local structural features of selected elements in heterogeneous catalysts. In particular, although the technique is actually a bulk technique it is also valuable for studying chemical reactions that take place at the surfaces of heterogeneous catalysts because the overall contribution to the XAS signal arises from the significant proportion of active sites that are highly dispersed over a large number of surfaces. XAS has been used extensively to study local metal environments in a number of zeotypes. Examples include metal-substituted microporous alumino- and silicoalumino-phosphates (AlPOs and SAPOs)[7,17,25] and the cations in ion-exchanged zeolites, *e.g.* the copper-containing zeolite deNO_x catalysts.[26]

We report here the results of studies on the synthesis of CuAPO-5 and its characterisation by XRD, SEM and XAS. In addition, the catalytic activity of this material towards the selective reduction of NO_x in the presence of NH_3 and O_2 was measured.

Experimental

Synthesis

The synthesis of CuAPO-5 was similar to that described by Muñoz *et al.*[14] The copper source, CuO (1.6 g), orthophos-

phoric acid (6.8 ml; H_3PO_4, 85 wt%, Merck) and deionised water (18.2 ml) were mixed and stirred until a blue solution was obtained (30 minutes). To this solution was added pseudo-boehmite (7.3 g; AlOOH, BA Chemicals Ltd.) (Muñoz *et al.* used alumina), and the mixture stirred until a homogenous gel formed (1.5 hour). At this stage the template, tetraethylammonium hydroxide (18 ml; TEAOH, 40%, Aldrich) was added and the gel stirred for another hour. The resulting turquoise-coloured gel (pH 3) was transferred into Teflon-lined stainless-steel bombs, and heated at 150 °C for 24 hours.

Crystallisation was accompanied by an increase in pH to 7. The crystalline, turquoise-coloured product was filtered, washed with deionised water and dried in air at room temperature. Samples of this material were calcined at 550 and 800 °C.

Another putative CuAPO-5 was prepared according to the above procedure but using copper acetate (2.0 g) instead of copper(II) oxide. The catalytic activities of the material derived from the oxide and the acetate were measured.

For the purpose of comparing the XANES, an ion exchanged Cu-β zeolite was prepared as described by Jensen.[27]

Characterisation

X-Ray powder diffractograms were obtained using a Siemens D-5005 diffractometer, equipped with a scintillation detector and Cu K_α radiation (Cu K_α being removed by a Ni filter). The copper content was determined by atomic absorption spectroscopy (AAS) on a Perkin Elmer 1100 B AAS using the flame technique.

Scanning electron micrography was performed on a Zeiss DSM 940 Scanning Electron Microscope. Elemental analyses were carried out using X-ray flourescence spectroscopy (Philips PW1480) by NGU (The Geological Survey of Norway).

X-Ray absorption data collection

XAS data were collected on the Swiss–Norwegian beamline (SNBL), station EH1, at the European Synchrotron Radiation Facility (ESRF) and on station 8.1 at the Daresbury Synchrotron Radiation Source (SRS) at the copper K-edge ($\lambda = 1.38043$ Å, $E = 8979$ eV).

Channel cut Si(111) and bent double crystal Si(220) monochromators were used to scan the X-ray spectra at the ESRF and SRS, respectively. Ion chambers were used at both facilities for detecting the intensities of the incident (I_0) and transmitted (I_t) X-rays. The detector gases at the ESRF were as follows: I_0, detector length 17 cm, 97.1% N_2, 2.9% Ar; I_t, length 31 cm, 49.5% N_2, 50.5% Ar. At SRS, the first ion chamber was filled with Ar at a partial pressure of 47 Torr and the second ion chamber with Ar at a partial pressure of 338.6 Torr, both being filled to atmospheric pressure with He. In both cases the gas mixtures account for 20% and 80% absorption in I_0 and I_t, respectively.

The experiments were performed with electron beam energies of 6.0 (ESRF) and 2.0 (SRS) GeV with maximum stored currents of 200 mA at both facilities.

At the ESRF, higher-order harmonics (*ca.* two orders of magnitude) were rejected by means of a gold-coated mirror angled at 7.3 mrad from a beam of size 0.6×4.7 mm which was defined by the slits in the station. The maximum resolution ($\Delta E/E$) of the Si(111) bandpass is 1.4×10^{-4}. At SRS, the harmonic rejection was set to 50%.

The amounts of material in the samples were calculated from element mass fractions and the absorption coefficients of the constituent elements[28] above the absorption edge to give an absorber optical thickness of 1.5 absorption lengths. The well-powdered (50–100 mg) samples were mixed with boron nitride so as to obtain a homogeneous sample thickness of *ca.* 1 mm for a surface area of 1.2 cm^2, placed in aluminium sample holders and held in place by Kapton tape windows. Several scans were collected and summed for each sample.

At the ESRF, XAS data were collected during reduction of a sample of CuAPO-5. Prior to reduction, the sample had been calcined in helium (5 °C min^{-1}) up to 500 °C and kept at this temperature for one hour. This pre-treated sample was then loaded into a Lytle *in situ* reactor cell[29] and reduced in a mixture of H_2 (5%) in He (purity; 99.995%: flow rate 60 ml min^{-1}) by heating from room temperature to 450 °C and maintaining at that temperature for six hours.

EXAFS data analysis

The data were corrected for dark currents, summed and background subtracted to yield the EXAFS function $\chi^{obs}{}_i(k)$ by means of the EXCALIB and EXBACK programs.[30] The edge positions were determined from the first inflection points of the derivative spectra. Model fitting was carried out with EXCURV90,[30] using curved-wave theory and *ab initio* phase shifts calculated within EXCURV90. The low energy cut-off for all samples was 30 eV, and the k^3 weighting scheme was used.

The copper(II) Tutton salt,[31] $[Cu(H_2O)_6]^{2+}$ in aqueous solution, copper(II) hydroxide[32] and copper(II) oxide[33] were used as model compounds to check the validity of the *ab initio* phase shifts and to establish the general parameters, AFAC and VPI.[34] These parameters were transferred to the analyses on the unknowns in order to reduce any residual systematic error in the multiplicities.

The EXAFS spectra were least squares fitted using k^1 and k^3 weighted data, in order to reduce coupling between N (multiplicity) and $2\sigma^2$ (Debye–Waller-type factor). Solutions common to both weightings schemes were chosen.[35]

The k^3 weighting scheme used in the refinement compensates for the diminishing photoelectron wave at higher k. All of the spectra were treated in exactly the same manner and the validity of the data reduction and fitting procedures was checked against the spectra of the reference compounds. The data were analysed over the range $k = 12$ Å^{-1} (10 Å^{-1} for the calcined CuAPO-5), and the refinement carried out to minimise the fit index (FI):

$$FI = \sum_i [k^3(\chi_i^{exp} - \chi_i^{calc})]^2$$

where χ_i^{exp} and χ_i^{calc} are the experimental and theoretical EXAFS respectively.[30]

In order to ensure that the results are meaningful, it is essential to identify the maximum number of independent parameters, N_{ind}, that can be varied in the EXAFS analysis. This is given by $N_{ind} = 2\Delta k \Delta R/\pi$ where Δk is the extent of the data in k-space and ΔR the range of distance being modelled.[36] For as-synthesised CuAPO-5, $\Delta k = 12$ Å^{-1} and $\Delta R = 1.21$ Å, and for the calcined CuAPO-5, $\Delta k = 10$ Å^{-1} and $\Delta R = 1.23$ Å. For these analyses, the maximum value corresponds to $N_{ind} = 9$ and 8, respectively. Another constraint is the smallest separation of shells that can be resolved. This is given by $\pi/\Delta k = 0.26$ Å for the as-synthesised and 0.31 Å for the calcined sample.[36] The addition of successive shells was tested for significance using the procedure of Joyner *et al.*[37]

NO conversion

The efficiency of CuAPO-5 in the selective reduction of nitric oxide to dinitrogen was measured as follows: NO (2000 ppm) in N_2 was mixed with NH_3 (1000 ppm) and O_2 and passed through the sample (*ca.* 50 mg) which was placed in a Pyrex reactor (10 mm internal diameter). The reactor was electrically heated to the given temperature. The NO conversion was determined by UV/VIS using the characteristic NO peak at 215 nm as a measure; the data were recorded on a Jasco V-570

UV/VIS spectrophotometer with a PC link. The conversion measurements were carried out over the temperature range 150–500 °C.

Results and discussion

Characterisation

The diffractograms (Fig. 1) confirm that the sample has the $AlPO_4$-5 (AFI) structure.[38] The material is thermally stable at 550 °C, but decomposes at 800 °C. The scanning electron micrograph of CuAPO-5 is shown in Fig. 2. The size of the particles, clusters of hexagonal crystals, is 10–20 μm. Analysis showed the composition to be $Cu_{0.2}AlP_{0.8}O_4$ with the copper content being 5.0%. Like Muñoz *et al.*[14] the analyses suggest that copper substitutes for phosphorus although this conclusion needs to be substantiated by other methods.

Copper coordination and colour

The structural interpretation of the EXAFS spectra has to be consistent with the colours of the different products. For the as-synthesised and calcined (550 °C and 800 °C) CuAPO-5 products, the colours are as follows: $CuO/AlOOH/H_3PO_4$, turquoise; as-synthesised, turquoise; calcined at 550 °C, grey; calcined at 800 °C, turquoise.

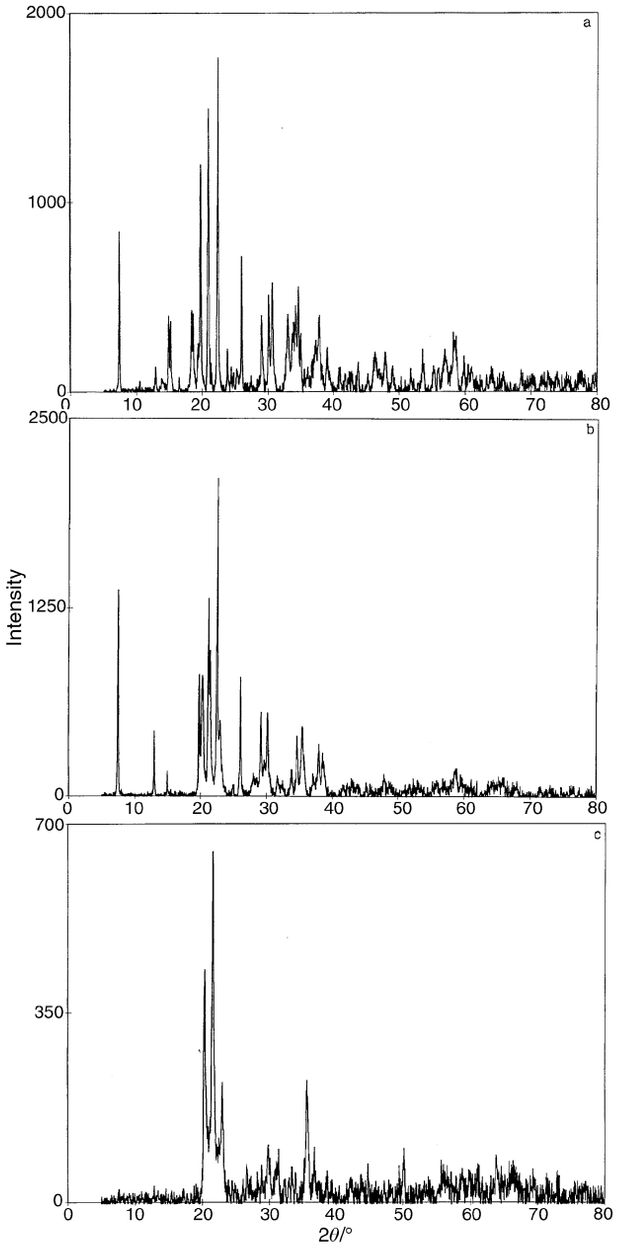

Fig. 1 X-Ray powder diffractograms of CuAPO-5 sample: (a) as-synthesised; (b) calcined at 550 °C; (c) calcined at 800 °C.

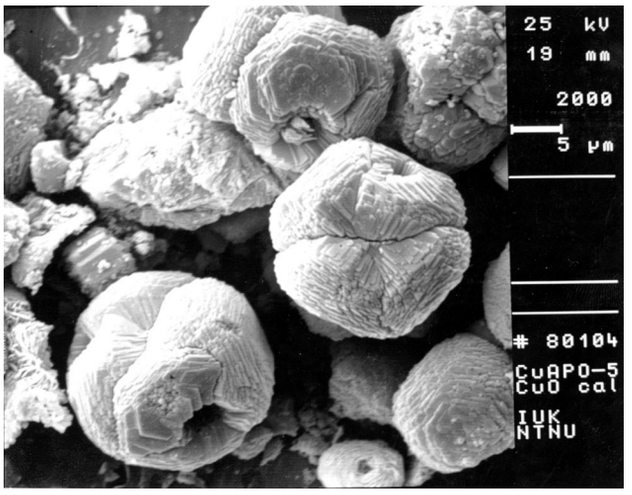

Fig. 2 Scanning electron micrograph of calcined CuAPO-5.

The turquoise colour is characteristic of tetragonally distorted $Cu(O)_6$ environments such as hydrated copper(II) cations,[39] copper(II) hydroxide[32] and the mineral turquoise itself ($CuAl_6(PO_4)_4(OH)_8 \cdot 4H_2O$).[40] However, although the colours are the same, the degree of tetragonal distortion varies widely (from 2.21 to 2.63 Å for the axial distances in the hydrated cation and in copper(II) hydroxide, respectively). Indeed, the copper environment in the hydroxide may be described as square planar if the long axial distances are ignored. This is also the case for copper oxide and the distinction between square planar and tetragonally distorted octahedral coordination is not clear.[41] Hence, in the present compounds the turquoise colour is consistent with both tetragonal six coordination and square planar four coordination and the EXAFS spectra were used to distinguish between these and other environments.

EXAFS analysis

The k^3-weighted experimental and least-squares fitted EXAFS spectra of the model compounds and the as-synthesised and calcined samples of CuAPO-5 are shown in Fig. 3 and 4. Also shown in the figures are the corresponding Fourier transforms. Tables 1 and 2 give the results of the least-squares analyses.

The models. The EXAFS spectra of the hexaaquacopper(II) cation in the Tutton salt and in aqueous solution together with copper(II) hydroxide and copper(II) oxide were satisfactorily fitted to crystallographic parameters.[31–33] The long axial (tetragonal distortion, see above) Cu–O distances in copper hydroxide and copper oxide (2.63 and 2.78 Å, respectively) are not readily apparent in the Fourier transforms. It is a general feature of tetragonally distorted octahedral copper(II) environments that the axial ligands are not clearly manifested in the EXAFS. Examples also include heavier ligands such as chloride.[42] This is attributed to a combination of large Debye–Waller-type factors and interference with oscillations from more distant shells. However, there are examples for which the axial distances are apparent. These have low Debye–Waller factors (see below).

It is of interest to compare the EXAFS of the $[Cu(H_2O)_6]^{2+}$ cation in the Tutton salt with the same cation in aqueous solution. Whereas the former is readily fitted to six Cu–O distances (represented by two (4 + 2) averaged distances) in the latter the axial water molecules are not resolved from the equatorial. It is known that a dynamic Jahn–Teller effect

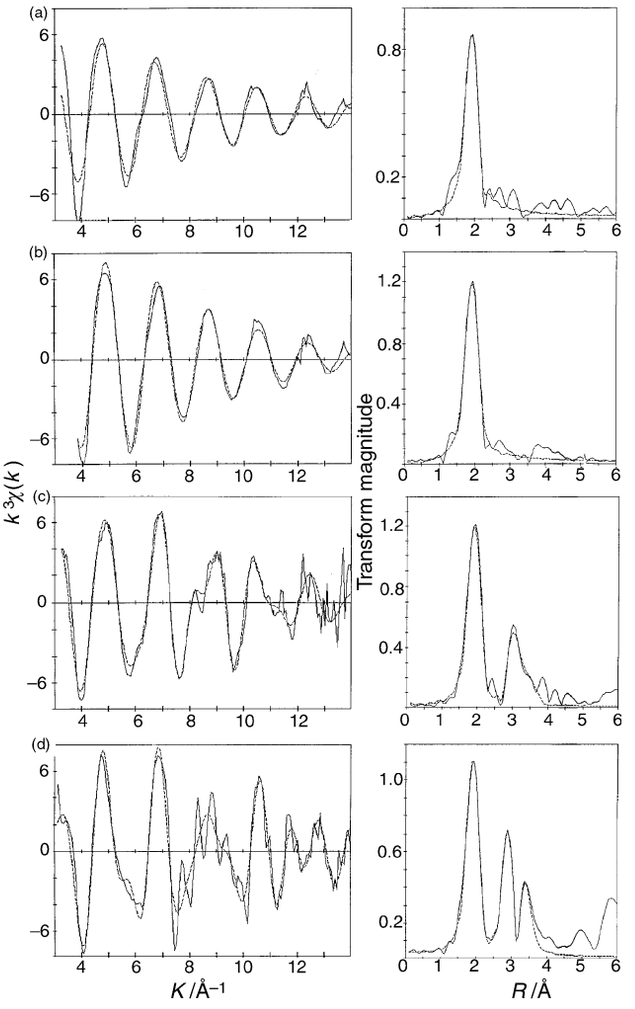

Fig. 3 Experimental (—) and calculated (---) Fourier filtered (1.0–25.0 Å) k^3-weighted EXAFS and their Fourier transforms for (a) copper(II) Tutton salt; (b) hexaaquacopper(II) ion; (c) copper(II) hydroxide and (d) copper(II) oxide.

applies here.[43,44] (The influence of crystal packing forces on the cation in the Tutton salt is mentioned below.)

CuAPO-5. The Fourier transform of the turquoise as-synthesised sample shows two distinct peaks. These were fitted to four Cu–O distances (1.93 Å), and four Cu···T (T = Al or P, see below) distances (3.13 Å). Judging by the model compounds any longer range axial distances (>2.5 Å) would not be readily apparent and the EXAFS is therefore consistent with a tetragonally distorted $Cu(O)_6$ environment and its attendant colour. Unlike the hexahydrated copper(II) cation in the Tutton salt which is readily fitted to a spread of six oxygen distances, the as-synthesised material shows four coordination. This implies that the axial distances in the latter are long (as mentioned above).

In the calcined sample, four Cu–O distances at 1.94 Å are found. In addition, there is a second Cu–O shell at 2.14 Å with a multiplicity of two. Attempts to fit a shoulder at *ca.* 2.7 Å on a peak at 3.1 Å to different backscatterers were unsuccessful. However, closer inspection (Fig. 4) shows that this shoulder is actually a feature arising from interference with three shells. The peak in the third shell was fitted to four Cu···T distances at 3.16 Å.

The four Cu–O distances of the as-synthesised and calcined samples are similar to those in the square-planar arrangement in copper hydroxide (see above) and in the elongated tetrahedron found in the zeolite pollucite analogue, $Cs_2CuSi_5O_{12}$.[45] The latter is of special interest because it is one of the few examples of tetrahedron-based copper(II) coordination.

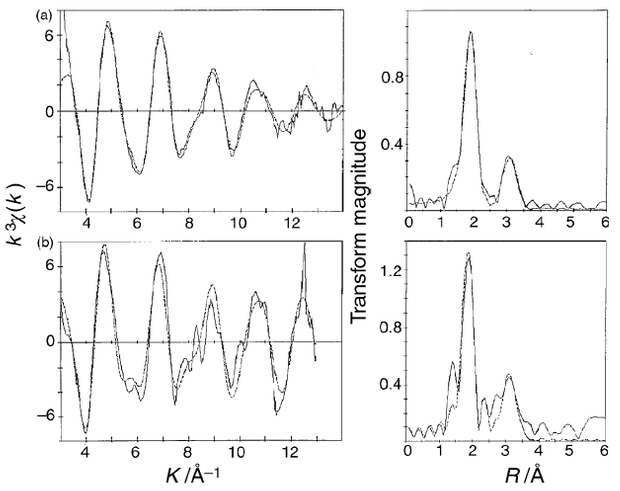

Fig. 4 Experimental (—) and calculated (---) Fourier filtered (1.0–25.0 Å) k^3-weighted EXAFS and their Fourier transforms for CuAPO-5: (a) as-synthesised sample; (b) calcined sample.

In general, substituting a metal (M) into some of the T sites of the zeotype lattice leads to four M···T distances of *ca.* 3.1 Å,[45] thereby providing a convenient indicator for framework substitution. The atomic numbers for the T atoms are too similar for EXAFS to unequivocally distinguish between them. Hence, aluminium was used to represent both T atoms. (If copper substitutes phosphorus then the four neighbouring T atoms are actually aluminium (see above).)

The EXAFS results, together with the colours of the as-synthesised and calcined materials (turquoise and grey), are consistent with tetragonal and non-tetragonal octahedra, respectively. For the latter, all six distances are clearly apparent, which is consistent with their relatively small Debye–Waller factors (see above for tetragonal distortion and high Debye–Waller factors). We have also observed[46] a tetragonally distorted octahedron in which the Debye–Waller factors are low and the axial distances are clearly resolved; this material is copper-incorporated SnAPO-5. It is also relevant to this work that the crystal structure of the same material shows that the axial bonds to copper are from lattice-bound oxygens.

The difference between the $Cu(O)_6$ environments of the as-synthesised and calcined materials can be rationalised in terms of varying degrees of integration of the copper atoms into the $AlPO_4$-5 lattice. For the as-synthesised material each copper atom is not fully integrated by being bound to the full complement of six framework oxygens and is therefore still free to adopt the turquoise tetragonally distorted octahedron in which the axial bonds are possibly to hydroxy groups. On calcination at 550 °C the colour changes as copper becomes fully integrated into the framework at the cost of its environment being degraded to an unspecified distorted octahedron, possibly a distorted tetrahedron with two additional longer bonds. These changes are accompanied by the change in colour from turquoise to grey. Calcination at 800 °C causes the $AlPO_4$-5 structure to break down and the resilience of the tetragonally distorted octahedron for $Cu(O)_6$ is demonstrated as the structural restraints imposed by the $AlPO_4$-5 lattice are removed and the colour reverts back to turquoise.

Muñoz *et al.*[14] presented electron spin resonance (ESR) and electron spin-echo modulation (ESEM) spectroscopic evidence for copper being incorporated into the framework of their CuAPO-5, and showed that framework-substituted copper(II) can achieve four-, five- or six-coordination, depending on the number of extraframework species coordinated to copper. These results, together with the EXAFS presented here, are

Table 1 Results of EXAFS curve-fitting (k-range: 3.0–15.0 Å^{-1}) for the model compounds[a]

Model		N[b]	r/Å (X-ray)[b]	r/Å	$2\sigma^2$/Å^2	E_0/eV	R (%)
$Cu(NH_4)_2(SO_4)_2{\cdot}6H_2O$	Cu–O	4.0	2.02	1.958(3)	0.010(1)	27.0(7)	26.0
(Tutton salt)	Cu–O	2.0	2.23	2.13(1)	0.026(4)		
$Cu(H_2O)_6^{2+}$	Cu–O	6.0	—	1.944(2)	0.013(1)	26.4(4)	19.0
$Cu(OH)_2$	Cu–O	4.0	1.94	1.941(2)	0.010(1)	25.3(3)	27.1
	Cu–O	2.0	2.63[c]	—	—		
	Cu···Cu	2.0	2.95	2.933(5)	0.018(1)		
	Cu···Cu	4.0	3.34	3.23(1)	0.034(3)		
CuO	Cu–O	4.0	1.96	1.940(2)	0.011(1)	23.0(3)	32.4
	Cu–O	2.0	2.78[c]	—	—		
	Cu···Cu	8.0	2.90	2.881(5)	0.028(1)		
	Cu···Cu	2.0	3.08	3.102(1)	0.011(1)		
	Cu···Cu	2.0	3.42	3.38(1)	0.022(3)		

[a]Each bonding distance (R) is associated with a coordination number (N) and thermal vibration and static disorder (Debye–Waller-like factor, $2\sigma^2$). E_0 is the refined correction to the threshold energy of the absorption edge. The standard deviation in the least significant digit as calculated by EXCURV90 is given in parentheses. However, note that such estimates of precision overestimate the accuracy, particularly in cases of high correlation between parameters. The estimated standard deviations for the distances are 0.01 Å at $R<2.5$ Å, with $\pm 20\%$ accuracy for N and $2\sigma^2$, although the accuracy for these is increased by refinements using k^1 *vs.* k^3 weighting (see main text). Residual index R was calculated as $R=\sum_i [(\chi_i{}^{exp}-\chi_i{}^{calc})k^{WT}]^2/\sum_i [(\chi_i{}^{exp})k^{WT}]^2$ [b]The fixed multiplicities and crystallographic distances are taken from references 31–33. [c]See main text.

consistent with a distorted tetrahedral environment with two longer, but relatively strong, interactions. However, we regard the environment as being distorted octahedral when the longer two distances are included. Because the bonding requirements for copper differ from those for phosphorus, there is a local distortion in the lattice about copper, which means that the two additional oxygens are framework oxygens.

XANES. Since it is known that the calcination of some copper(II) zeolites leads to the autoreduction of copper(II) to copper(I) (examples include Cu-ZSM-5[26] and Cu-β zeolite—see below), it is important when studying the catalytic properties to establish whether or not this behaviour also extends to the present copper-containing zeotype.

XANES spectra are convenient indicators of autoreduction because copper(I) spectra contain a characteristic intense pre-edge feature a few electronvolts below the edge (at *ca.* 8983–8986 eV).[47,48] (A detailed discussion on the dependence of the pre-edge peak intensity on the local copper(I) coordination is given by Moen *et al.*[49]) This is illustrated in Fig. 5 which shows the XANES regions for the diamminecopper(I) cation and copper(I) oxide. The first derivatives of the edge regions (Fig. 5) are also shown because they are useful for establishing transition energies and, in particular, highlighting characteristic features.[17] This is nicely illustrated by the derivative spectra of the $[Cu(H_2O)_6]^{2+}$ ion in the Tutton salt and in aqueous solution (Fig. 5). The considerable differences between the two spectra are attributed to the effects of crystal packing forces on the cation in the Tutton salt.

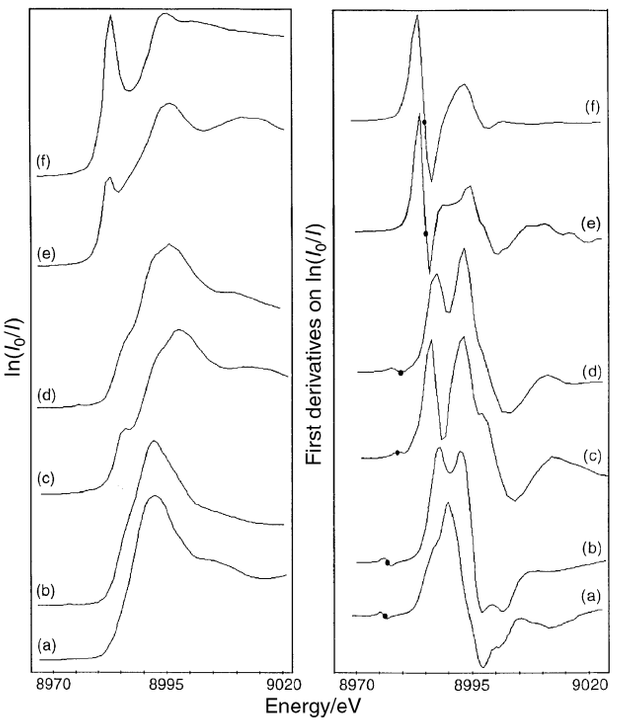

Fig. 5 Normalised Cu K-edge XANES and the first derivatives of (a) copper(II) Tutton salt; (b) hexaaquacopper(II) ion; (c) copper(II) oxide; (d) copper(II) hydroxide; (e) copper(I) oxide; (f) copper(I) diammine ion.

It is clear from the XANES (particularly the first derivative spectra) of the present materials (Fig. 6) that autoreduction does not occur. This conclusion is supported by the very weak transition at 8979 eV (the formally dipole-forbidden 1s→3d transition) that is characteristic of copper(II) compounds.[47] This transition is most intense when the first coordination shell

Table 2 Results of EXAFS curve-fitting for CuAPO-5.[a] k-ranges: as-synthesised sample: 3.0–15.0 Å^{-1}; calcined sample: 3.0–13.0 Å^{-1}

Sample		N[b]	r/Å	$2\sigma^2$/Å^2	E_0/eV	R (%)
As-synth.	Cu–O	4.0	1.922(1)	0.012(1)	21.3(2)	17.9
	Cu···Al[c]	4.0	3.131(4)	0.024(1)		
Calc.	Cu–O	4.0	1.937(3)	0.006(1)	13.6(4)	33.2
	Cu–O	2.0	2.147(8)	0.010(2)		
	Cu···Al[c]	4.0	3.164(8)	0.018(2)		

[a]See footnote *a* of Table 1 for details. [b]The multiplicities are fixed in the final refinements at the integer closest to the values returned by the full refinements. [c]See text.

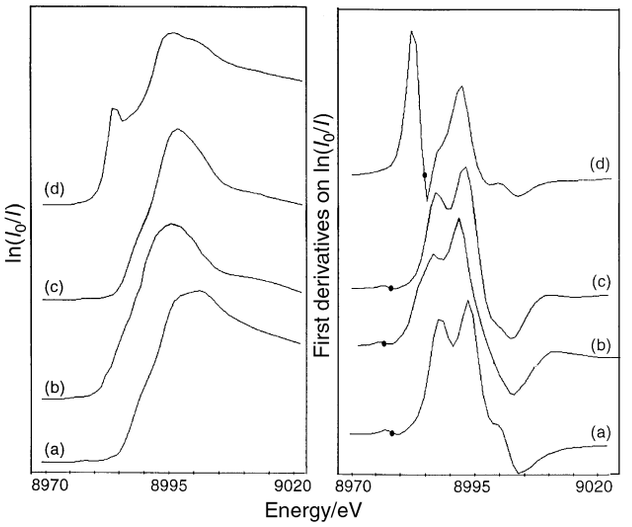

Fig. 6 Normalised Cu K-edge XANES and the first derivatives of (a) as-synthesised CuAPO-5; (b) calcined CuAPO-5; (c) as-synthesised Cu-β; (d) calcined Cu-β.

lacks inversion symmetry, which is the case for tetrahedral (T_d) environments but not octahedral (O_h) or tetragonal (D_{4h}) environments. Since the examples of autoreduction are associated with ion-exchanged zeolites the low intensity of this transition is consistent with framework copper(II) and that the environment is tetragonal rather than tetrahedral.

Also characteristic for tetragonal copper(II) complexes is a transition manifested by a shoulder or peak about halfway up the absorption edge. This is attributed to the 1s→4p transition accompanied by ligand-to-metal charge transfer and shake-down transitions.[23,42,50] In the XANES of copper(II) oxide (Fig. 5), this transition is present as a prominent shoulder at 8991 eV. The XANES of CuAPO-5 (Fig. 6) does not show this shoulder, hence copper(II) oxide is absent in the sample.

Reduced CuAPO-5. Since there is a general consensus that all zeolite-exchanged copper species are reduced by hydrogen to metallic copper,[51] we wanted to ascertain whether framework copper behaves similarly.

The XANES spectra and the Fourier transform of the EXAFS of the reduced CuAPO-5 material compared to Cu-foil are depicted in Fig. 7. The similarity between the spectra of CuAPO-5 and copper metal shows that copper in CuAPO-5 has been completely reduced to the bulk metal (*i.e.* particle dimensions >40 Å)[52] under these conditions. Hence, reducibility does not distinguish between framework and extraframework copper.

NO conversion. The results of the catalytical behaviour of CuAPO-5 towards the conversion of NO to N_2 with NH_3 are

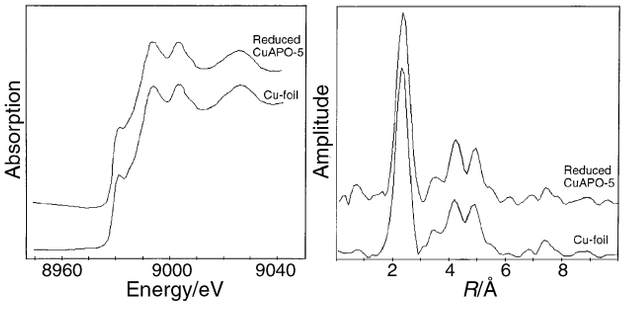

Fig. 7 XANES spectra at the Cu K-edge and the Fourier transforms (1.0–25.0 Å) of the EXAFS for metallic copper and CuAPO-5, reduced in H_2/He.

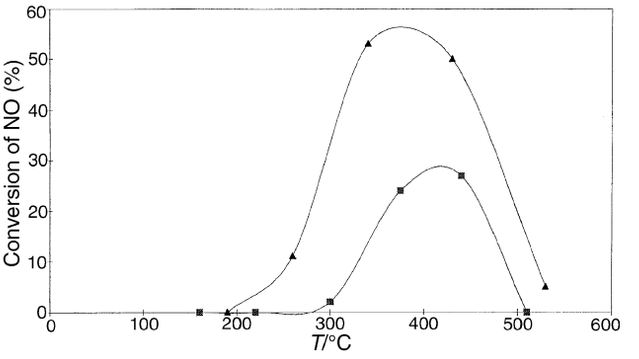

Fig. 8 Catalytic activity of CuAPO-5 for the selective catalytic reduction of NO_x in the presence of NH_3 and O_2. ■: Sample A; copper(II) as copper source. ▲: Sample B; copper(II) acetate as copper source.

shown in Fig. 8. CuZSM-5[22] and to a lesser degree CuAPO-5/$CuAc_2$ show higher maxima at lower temperatures (100% at 200–300 °C and 53% at 340 °C, respectively) than CuAPO-5/CuO (27% at 430 °C) for the conversion. The different catalytic behaviour shown by the three materials may possibly be related to the different copper environment (*i.e.* framwork, ion-exchanged and extra-framework,[46] respectively).

For comparison, the activity towards NO of a mixture of $AlPO_4$-5 and CuO (5.0% copper) was measured. This mixed sample exhibits no activity, a result which also shows that copper is not present as copper(II) oxide in the CuAPO-5 samples (see above).

Conclusion

(i) The decreases in the Al : P ratio of CuAPO-5 indicate that copper is incorporated into the framework of the zeotype and it would appear that this substitution occurs at phosphorus sites. Structural support for framework substitution is given by the EXAFS of the as-synthesised and calcined materials and by the ESR study by Muñoz *et al.*[14] Interpretation of these structural parameters is consistent with the colours of the products. In the turquoise as-synthesised materials the copper environments are tetragonally distorted octahedra in which the axial positions are possibly occupied by hydroxy groups. In the grey calcined material (550 °C) coordination to the framework is increased by a further two bonds to framework oxygen atoms and the symmetry degrades from a tetragonally distorted octahedron to a non-tetragonally distorted octahedron for which the coordination is increased from distorted tetrahedral by two longer bonds to framework oxygens. On further calcination (800 °C) the microporous structure breaks down and copper is free to reassert its preference for the tetragonal octrahedral environment and a turquoise colour. (ii) The XANES spectra of the Cu-β zeolite and CuAPO-5 show that the latter differs from the copper ion-exchanged zeolite in not undergoing autoreduction. (iii) XANES and EXAFS show that copper(II) in CuAPO-5 is reduced to large particles (>40 Å) upon reduction in hydrogen. (iv) CuAPO-5 is a relatively poor catalyst for reducing NO in the presence of NH_3 and O_2. However, putative CuAPO-5 synthesised from copper(II) acetate is a significantly better catalyst.

Acknowledgements

Support from the Nansen Foundation and VISTA-Statoil (to D.G.N.) is much appreciated. We thank the Norwegian University of Science and Technology and the Norwegian Research Council for grants towards the construction of the Swiss-Norwegian Beamline (SNBL). The assistance of the SNBL Project Team (W. van Beck, H. Emerich, K. Knudsen,

P. Pattison and H.P. Weber) and L.M. Murphy at station 8.1 (SRS) is much appreciated. R. Fehrmann, C. B. Nielsen and R. Mattsson at the Department of Chemistry, the Technical University of Denmark (DTU) are thanked for assistance with the catalytical measurements.

References

1 B. M. Lok, C. A. Messina, R. L. Patton, R. T. Gajek, T. R. Cannan and E. M. Flanigen, *J. Am. Chem. Soc.*, 1984, **106**, 6092.
2 C. Halik, J. A. Lercher and H. Mayer, *J. Chem. Soc., Faraday Trans.*, 1988, **84**, 4457.
3 N. Ulagappan and V. Krishnasamy, *J. Chem. Soc., Chem. Commun.*, 1995, 373.
4 K. J. Chao, A. C. Wei, H. C. Wu and J. F. Lee, *Catal. Today*, 1999, **49**(1–3), 277.
5 Z. D. Zhu and L. Kevan, *Phys. Chem. Chem. Phys.*, 1999, **1**, 199.
6 C. M. Cardile, N. J. Tapp and N. B. Milestone, *Zeolites*, 1990, **10**, 90.
7 P. A. Barrett, G. Sankar, C. R. A. Catlow and J. M. Thomas, *J. Phys. Chem.*, 1996, **100**, 8977.
8 Y. Xu, J. W. Couves, R. H. Jones, C. R. A. Catlow, G. N. Greaves, J. Chen and J. M. Thomas, *J. Phys. Chem. Solids*, 1991, **52**, 1229.
9 G. Sankar, J. M. Thomas, J. Chen, P. A. Wright, P. A. Barrett, G. N. Greaves and C. R. A. Catlow, *Nucl. Instrum. Methods Phys. Res. B*, 1995, **97**, 37.
10 G. Lischke, B. Parlitz, U. Lohse, E. Schreier and R. Fricke, *Appl. Catal. A: Gen.*, 1998, **166**, 351.
11 N. J. Tapp and C. M. Cardile, *Zeolites*, 1990, **10**, 680.
12 N. Rajic, D. Stojakovic and V. Kaucic, *Zeolites*, 1991, **11**, 612.
13 A. Moen and D. G. Nicholson, *J. Chem. Soc., Faraday Trans.*, 1995, **91**, 3529.
14 T. Muñoz Jr, A. M. Prakash, L. Kevan and K. J. Balkus Jr, *J. Phys. Chem. B*, 1998, **102**, 1379.
15 G. Hutchings, *Chem. Br.*, 1992, **28**(11), 1006.
16 J. M. Thomas, *Angew. Chem., Int. Ed. Engl.*, 1994, **33**, 913.
17 A. Moen, D. G. Nicholson. M. Rønning, G. M. Lamble, J.-F. Lee and H. Emerich, *J. Chem. Soc., Faraday Trans.*, 1997, **93**, 4071.
18 M. Iwamoto, H. Furukawa, Y. Mine, F. Uemura, S. Mikuriya and S. Kagawa, *J. Chem. Soc., Chem. Commun.*, 1986, 1272.
19 M. Iwamoto and H. Hamada, *Catal. Today*, 1991, **10**, 57.
20 G. Centi and S. Perathoner, *Appl. Catal. A: Gen.*, 1995, **132**, 179 and references cited therein.
21 M. Wark, A. Brückner, T. Liese and W. Grünert, *J. Catal.*, 1998, **175**, 48.
22 G. Centi, C. Nigro, S. Perathoner and G. Stella, *Catal. Today*, 1993, **17**, 159.
23 E. Y. Choi, I.-S. Nam, Y. G. Kim, J. S. Chung, J. S. Lee and M. Nomura, *J. Mol. Catal.*, 1991, **69**, 247.
24 J. W. Byrne, J. M. Chen and B. K. Speronello, *Catal. Today*, 1992, **13**, 33.
25 S. Thomson, V. Luca and R. Howe, *Phys. Chem. Chem. Phys.*, 1999, **1**, 615.
26 D.-J. Liu and H. J. Robota, *J. Phys. Chem. B*, 1999, **103**, 2755.
27 S. F. Jensen, Ph. D. Thesis, The Norwegian University of Science and Technology, The Department of Industrial Chemistry, 1998.
28 *International Tables for X-Ray Crystallography*, The Kynoch Press, Birmingham, UK, 1962, vol. 3, p. 175.
29 F. W. Lytle, R. B. Greegor, E. C. Marques, D. R. Sandstrom, G. H. Via and J. H. Sinfelt, *J. Catal.*, 1985, **95**, 546.
30 N. Binsted, J. W. Campbell, S. J. Gurman and P. C. Stephenson, EXCALIB, EXBACK and EXCURV90 programs, SERC Daresbury Laboratory, 1990.
31 G. M. Brown and R. Chidambaram, *Acta Crystallogr., Sect. B*, 1969, **25**, 676.
32 H. Jaggi Von and H. R. Oswals, *Acta Crystallogr.*, 1961, **14**, 1041.
33 S. Åsbrink and L.-J. Norrby, *Acta Crystallogr., Sect. B*, 1970, **26**, 8.
34 S. J. Gurman, N. Binsted and I. Ross, *J. Phys. Chem. C*, 1984, **17**, 143.
35 F. W. H. Kampers, C. W. R. Engelen, J. H. C. van Hooff and D. C. Koningsberger, *J. Phys. Chem.*, 1990, **94**, 8574.
36 *Report on the International Workshops on Standards and Criteria in XAFS in X-ray Absorption Fine Structure*, ed. S. S. Hasnain, Ellis Horwood, Chichester, 1991, p. 751.
37 R. W. Joyner, K. J. Martin and P. Meehan, *J. Phys. C: Solid State Phys.*, 1987, **20**, 4005.
38 J. M. Bennett, J. P. Cohen, E. M. Flanigen, J. J. Pluth and J. V. Smith, *ACS Symp. Ser.*, 1983, **218**, 109.
39 J. D. Lee, *Concise Inorganic Chemistry*, 4th edn., Chapman and Hall, London, 1991, p. 827.
40 H. Cid-Dresdner, *Z. Kristallogr.*, 1965, **121**, 87.
41 N. N. Greenwood and A. Earnshaw, *Chemistry of the Elements*, Pergamon Press, Oxford, 1984, p. 1382.
42 I. J. Pickering and G. N. George, *Inorg. Chem.*, 1995, **34**, 3142.
43 K. Ozutsumi and T. Kawashima, *Polyhedron*, 1992, **11**, 169.
44 J. Garcia, M. Benfatto, Cr. Natoli, A. Bianconi, A. Fontaine and H. Tolentino, *Chem. Phys.*, 1989, **132**(1–2), 295.
45 A. R. Heinrich and Ch. Baerlocher, *Acta Crystallogr., Sect. C*, 1991, **47**, 237.
46 M. H. Nilsen, Ph.D. thesis, Norwegian University of Science and Technology, Department of Chemistry, 2000, to be submitted.
47 L.-S. Kau, D. J. Spira-Solomon, J. E. Penner-Hahn, K. O. Hodgson and E. I. Solomon, *J. Am. Chem. Soc.*, 1987, **109**, 6433.
48 G. Lamble, A. Moen and D. G. Nicholson, *J. Chem. Soc., Faraday Trans.*, 1994, **90**, 2211.
49 A. Moen, D. G. Nicholson and M. Rønning, *J. Chem. Soc., Faraday Trans.*, 1995, **91**, 3189 and references cited therein.
50 S. E. Shadle, J. E. Penner-Hahn, H. J. Schugar, B. Hedman, K. O. Hodgson and E. I. Solomon, *J. Am. Chem. Soc.*, 1993, **115**, 767.
51 T. Beutel, J. Sárkány, G.-D. Lei, J. Y. Yan and W. M. H. Sachtler, *J. Phys. Chem.*, 1996, **100**, 845.
52 M. Borowski, *J. Phys. IV*, 1997, **7**, 259.